

## Study on Crack Branching of 2324-T39 Aluminum Alloy under Tension Dominated Spectrum Loading

Ting Zhang<sup>1</sup>, Rui Bao<sup>1</sup>, Peiyong Liu<sup>2</sup>, Binjun Fei<sup>1</sup>

<sup>1</sup>School of Aeronautic Science and Engineering, Beihang University, 37 Xueyuan Road, Haidian District, Beijing, 100191, China

<sup>2</sup>School of Materials Science and Engineering, Beihang University, 37 Xueyuan Road, Haidian District, Beijing, 100191, China

Fatigue crack growth test of aluminum alloy 2324 was conducted with middle crack tension specimen in L-T orientation under truncated loading spectra. Since it is the case of sheet loaded uniaxially and tension dominated, the crack was expected to appear flat in global scale and normal to the loading direction. It is true for the low truncation level cases, however, significant crack branching was observed during the tests under high truncation levels. The factors which tends to result in crack branching are studied. Macro and Micro level investigation show that: 1) there are little inclusion in the alloy, therefore, the branching is not caused by the lack of homogeneity; 2) the appearance of crack branching has close relation with the tension overload although it cannot be observed immediately after the peak load; 3) the growth of subsurface secondary crack under high truncation levels is the main reason for surface crack branching, the occurrence of the secondary crack results from the tension overload, while the growth of the secondary crack depends on the interval of two peak loads.

**Keywords:** aluminum alloy 2324, fatigue crack growth, crack branching, spectrum loading

### 1. Introduction

Aluminum Alloy (AA) 2324-T39 plate, developed by ALCOA, is a higher strength version of alloy 2024-T351 and is a high-purity controlled composition variant of alloy 2024. It was developed for tension-dominated, fatigue and fracture critical plate applications and now is being used successfully on lower wing skin and center wing box components of new commercial transport aircraft [1]. Although the basic mechanical and fatigue performance of AA 2324 are given in [1], the fatigue and crack growth behaviors of this alloy is still widely investigated [2-4] due to its different characteristics with AA 2024. The crack growth behavior under truncated spectrum loading is one of the aspects attracting academic focus because low-load range truncation is a common practice in the full scale fatigue test of aircraft structural components, however, the elimination of low range cycles will, sometimes, change crack growth behavior. Studies on fatigue and fracture of ductile metals indicate that irrespective of the initial crack orientation, a fatigue crack tends to grown in Mode I and the favorable direction is perpendicular to the greatest local tensile stress [5]. The main concern in the study of crack growth under spectrum loading is the interactive effect of load sequence on crack growth rate [6]. No published literature shows that the elimination of small tension loading cycles would result in crack path change. However, during the experiments of crack growth in AA 2324 under truncated spectrum loading, which were originally designed to select a suitable low-load truncation level for the full scale fatigue test, it has been found that significant crack meandering or branching appeared when the load truncation level is increased to a certain value. The load truncation effects on crack growth life and crack growth rate were reported in [3, 7]. This paper presents the studies on the relationship between crack branching and fracture mechanism.

### 2. Material and Experiments

## 2.1 Material

The material studied in this paper is 2324-T39. The chemical composition limits is given in Table 1, compared with 2024. AA 2324 is not only the high-purity version of 2024 represented by the significant reduction of impurity substance Fe and Si, but also the upper limit for alloy element Cu is reduced. The reduction of Fe, Si and Cu results in the decrease of insoluble inclusion phases, e.g.  $Mg_2Si$ ,  $Al_{12}(FeMn)_3Si$ ,  $Al_7CuFe$ , etc., the appearance of surplus-phase  $CuAl_2$  is restricted at the same time [8]. Therefore, 2324 shows better fatigue and fracture performances compared with 2024. The high-purity controlled composition also results in the increase in grain size.

The T39 thermal treatment method increases the mechanical properties as well. The strength, fatigue performance and fracture toughness are about 5-16% higher than 2024-T351, furthermore, the increase in yield strength is 28%. The details of the mechanical properties are given in Table 2.

Table1 Chemical composition limits of AA 2324 and 2024

Alloy	Alloy elements				Impurity substance (%)					Others(%)	
	Cu	Mg	Mn	Al	Fe	Si	Zn	Ti	Cr	each	total
2324	3.8~4.4	1.2~1.8	0.3~0.9	Remainder	0.12	0.10	0.25	0.15	0.10	0.05	0.15
2024	3.8~4.9	1.2~1.8	0.3~0.9	Remainder	0.5	0.5	0.25	-	0.10	0.05	0.15

Note: value maximum if range not shown

Table2 Mechanical properties of 2324-T39 and 2024-T351 (L-T)

Alloy	Tensile Strength (MPa)	Yield Strength (MPa)	Elongation (%)	$K_{IC}$ (plane strain) ( $MPa\sqrt{m}$ )
2324-T39	475	370	8	38.5-44 (t = 19.05-33.02mm)
2024-T351	435	290	8	34 (t = 12.70-25.40mm)

## 2.2 Experiments

The FCG test was conducted with middle-crack tension, M(T), specimen. The configuration of the specimen is given in Fig.1. All the specimens are in L-T orientation, i.e. the applied external load is along the longitudinal (rolling) direction and the crack propagates along the transverse direction.

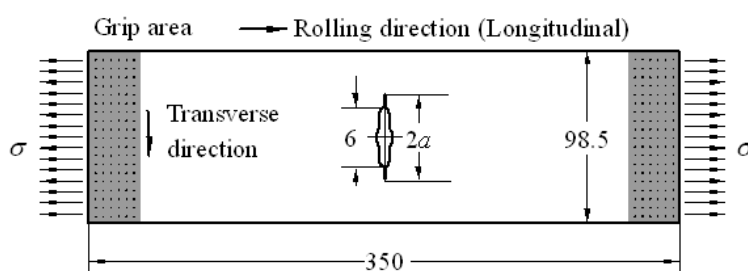


Fig.1 Configuration of the M(T) specimen (mm)

Six kinds of load spectra are employed in the FCG tests. The baseline load spectrum is a flight-by-flight spectrum containing five flight types arranged randomly within each load block. The baseline spectrum (S0) was filtered by removing small stress range cycles to obtain different truncated spectra. There are five truncation levels, 9.82%, 11.72%, 13.98%, 17.11% and 21.36%, resulting in five different truncated load spectra, named as S1, S2, S3, S4 and S5. A 9.82% truncation level indicates that those load cycles with stress range less than 9.82% of the maximum stress range in the S0 were removed, while the other parts of the spectrum were kept unchanged. The eliminated cycles in each loading block corresponding to the five truncation levels are 26.56%, 46.87%, 62.95%, 73.35% and 78.58% respectively. Segments of the loading cycles corresponding to the baseline

spectrum and the 5<sup>th</sup> truncation level are illustrated in Fig. 2. Both the baseline and truncated spectra are dominated by tension loads. The FCG tests were accomplished using the MTS 880 fatigue test system.

The fracture surfaces were cut from the specimens for micro-level investigation. Firstly, the crack paths were observed with universal measuring microscope; then the fracture surfaces were studied using scanning electron microscope (SEM) to obtain the microscopic fracture behavior; the surfaces of the specimen were also inspected with an optical microscope for understanding the micro structural characteristics.

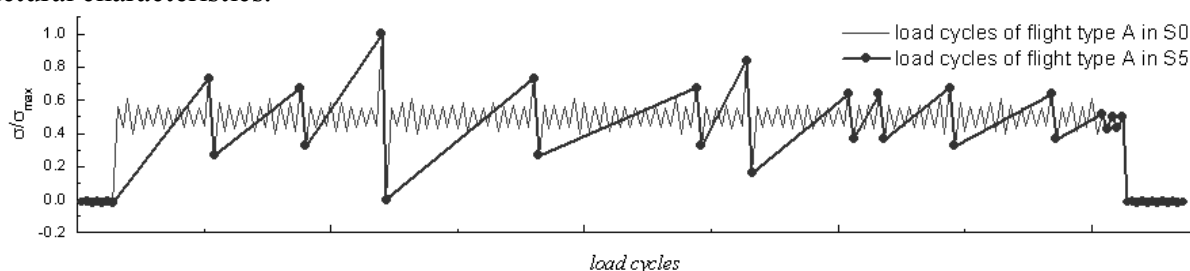


Fig.2 Segment of baseline and truncated loading spectrum

### 3. Macro-level crack morphology

It has been observed during the experiment that cracks subjected to the baseline load spectrum S0 and low truncation level S1, S2 and S3 are perfect mode I cracks which are flat and straight and perpendicular to the applied loads direction. A typical mode I crack occurred under spectrum S1 is illustrated in Fig. 3(a). However, significant crack meandering and/or branching are observed when the low-load range truncation is increased to a certain level, i.e. S4 and S5. A typical branched crack occurred under spectrum S4 and S5 is illustrated in Fig. 3(b) and (c).

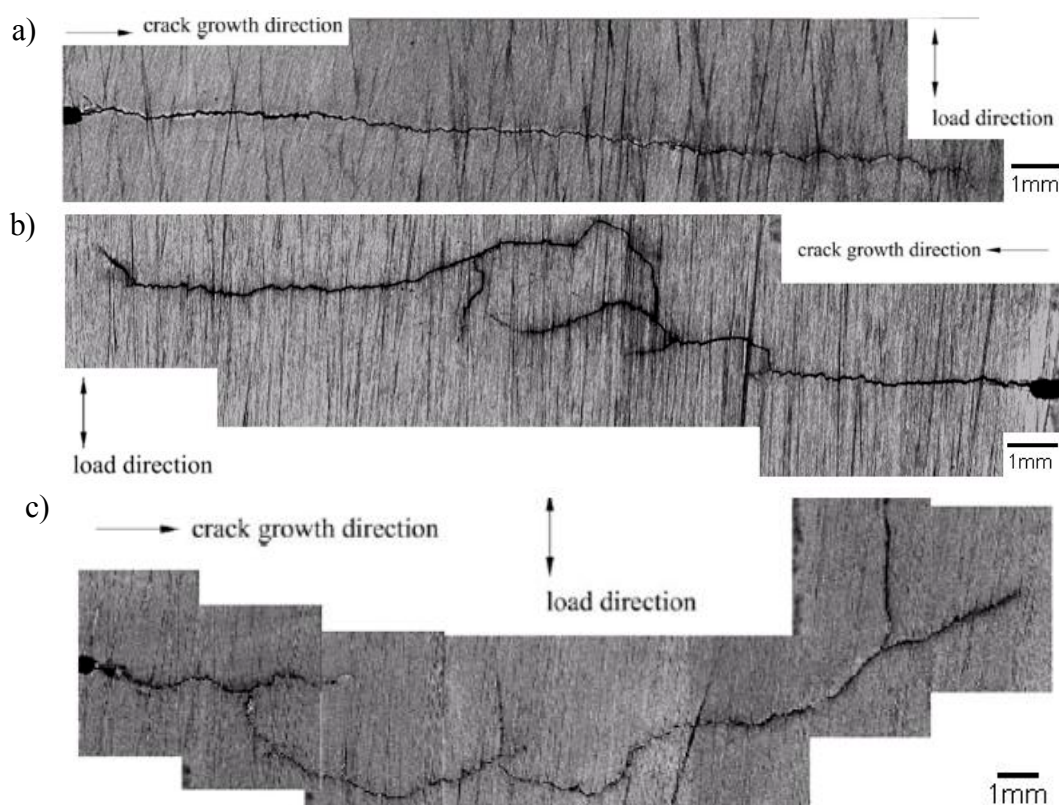


Fig. 3 Macroscopic crack morphology under (a) low truncation level S1, (b) high truncation level S4 and (c) S5

The significant crack branching is not resulted directly from the propagation of small branched crack. Surface secondary cracks were observed during the experiments and both the lead crack and the secondary cracks kept growing for a period of loading cycles until linked up, which has resulted in the observed remarkable crack branching. The appearance of the surface secondary cracks and the linking up process are shown in Fig. 4. No evidence shows that the surface secondary cracks initiate from the surface defects, they may raise from the growth of the subsurface secondary cracks.

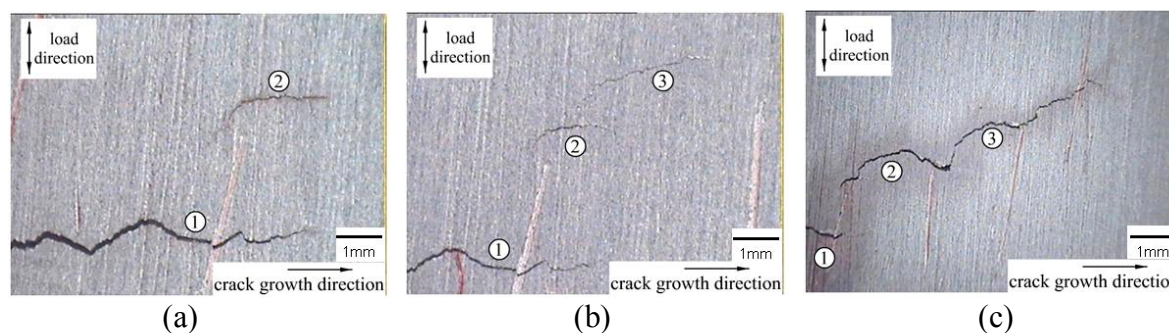


Fig. 4 Appearance of secondary surface cracks and cracks linking up

## 4. Microscopic investigation

### 4.1 Micro structure inspection

The micro structure inspection is aiming to find out if the homogeneity is the reason for crack branching. Two specimens are studied here, one is tested under S1 with no crack branching (in Fig. 3a), the other is tested under S5 with significant crack branching (in Fig. 3b). Fig. 5 (a) and (b) are the pictures taken by optical microscope for the two specimens, respectively. It can be seen from Fig. 5 that there is no noticeable difference in homogeneity of the two specimens. Therefore, the branched cracks are not caused by inhomogeneity of the material.

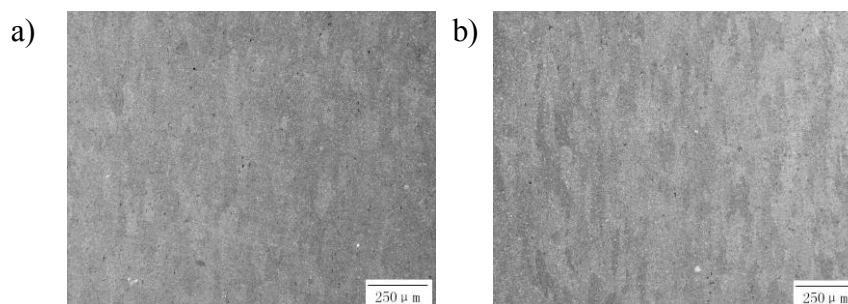


Fig.5 Micro structure of the two specimens (a) tested under S1 with no crack branching; (b) tested under S4 with significant crack branching

### 4.2 Fractographical investigation

The fracture surfaces from three specimens, cracked under S1, S4, and S5 respectively, are scanned with SEM. These three specimens are marked with M1, M2 and M3.

M1 is the specimen tested under S1 with truncation level of 9.82%. The crack, Fig. 3 (a), is flat in global scale and basically perpendicular to the applied tension load. The fracture surface under SEM shows typical fatigue failure characteristics, i.e. the striations as shown in Fig. 6 (a). Secondary cracks has been observed in Fig. 6(a), however, the secondary cracks remain in subsurface during the whole crack propagation procedure showing no influence on the global crack morphology.

M2 is the specimen tested under spectrum S4 with truncation level of 17.11%. Observing macroscopically from the surface of the specimen, the crack on the right hand side of the symmetric line of the specimen is perfect Mode I crack which is flat and perpendicular to load direction; whereas,

the crack on left hand side show remarkable branching which is no longer perpendicular to load direction, moreover, some of the branches are parallel to the applied tension load, see Fig. 3(b). Examination of the fracture surface of the branched side with SEM, Fig. 6(b), shows large areas containing plastic zone, having their edges with secondary cracks. These subsurface secondary cracks grow to the specimen surface leading to the macro-level crack branching. The growth of the main crack shows typical fatigue fracture feature. Fig. 6(c) shows the intersection of the plastic zone edges with the main crack, which results in the combined features of fatigue and ductile fracture.

M3 is the specimen tested under spectrum S5 with truncation level of 21.36%. Significant crack branching, Fig. 3(c), on both the sides of the middle crack was observed on the surface of the specimen during the FCG test. SEM investigation of the fracture surface shows combined fatigue and ductile fracture features, similar to the left hand side of M2.

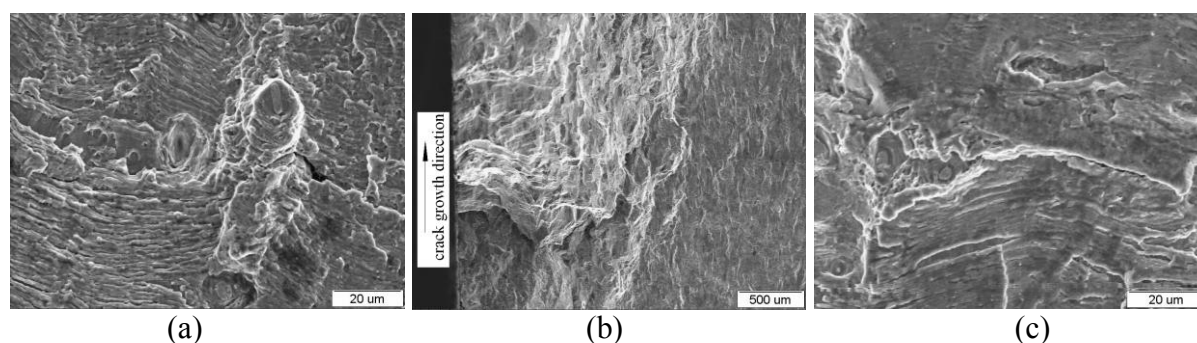


Fig. 6 Fractographic results of the specimens (a) tested under S1; (b) tested under S4; (c) tested under S5.

#### 4.3 Microscopic fracture mode

The surface of the specimen was scanned with optical microscope and SEM to identify the fracture mode of the branched crack as shown in Fig. 7. The main crack is typical transgranular fracture, while the branches show transgranular or transgranular shear fracture features.

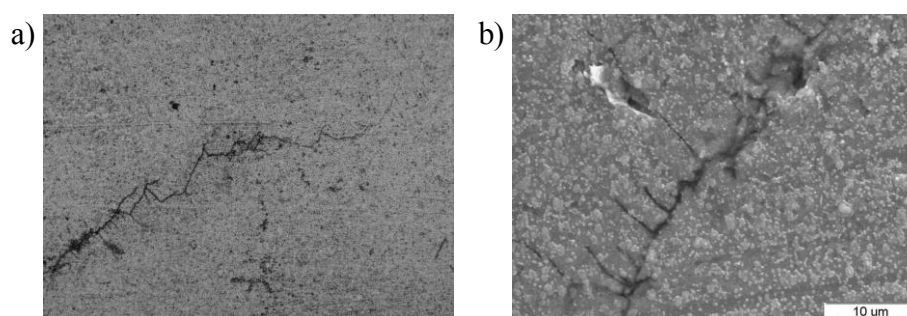


Fig. 7 Microscopic fracture features observed by (a) optical microscope and (b) SEM

## 5. Discussion

### 5.1 Relation of macroscopic crack branching and load history

From the aforementioned macro and micro investigations, it is clear that: 1) macroscopic crack branching was not initiated from the surface of the specimen (see Fig. 4); 2) surface crack branching is resulted from the coalescence of the main crack with the subsurface secondary crack which keeps growing to the specimen surface; 3) the existence of subsurface secondary crack is irrespective to load truncation level; 4) the difference is that secondary crack remains in subsurface under low truncation levels, on the contrary, it grows to the specimen surface under high truncation levels. The difference in load history of low and high truncation levels is that the loading cycles between the two peak tension load points. The loading cycles between the two peak loads are 197513, 71683 and 57593 for S1, S4 and S5, respectively. The value of the peak loads in all the load spectra is the same.

It can be deduced that the occurrence of the subsurface secondary crack is owing to the peak tension loads, while the subsurface secondary crack grows or not is depend on the interval of the two peak loads. If there are plenty of low-range loading cycles exist after one tension overload which results in a subsurface secondary crack, the crack tip of the main crack will be away from the secondary crack when the next overload comes, hence, the secondary crack keeps in limit length and remains in subsurface.

## 5.2 Growth mechanism of main crack and microscopic secondary crack

The growth mechanism of the crack in ductile metal is well known [5, 6] and the growth of the main crack in this study is typical. Although the mode I crack is flat in macro-level, however, on a microscopic scale, the main fracture surface is irregular with numerous interconnected micro-cracks intersecting the main crack; some of the cracks are even at nearly 90° to the main fracture [5]. These micro-cracks nucleates in the high-stress regions ahead of the crack and then interact with the main crack and ‘escape’ out of the plane of the main crack by micro-branching or micro-bifurcation because of changes in the distribution of stresses around the rapidly propagating crack [9].

The interaction between the micro-cracks with the main crack depends on the kinetics of growth of deformation zones and cracks. These, in turn, are related to the stress levels at which they are activated. In most cases, the micro-cracks grow a short distance resulting in steps between the main crack and the micro-cracks which will not leads to the macro-level crack path changes. However, in the specified high truncation level, the micro-cracks caused by one peak load will still in the high-stress region when the next overload comes, the growth of the micro-crack will not limited to a short distance. Macro-level crack branching appears when the final length of micro-crack is in a magnitude compared with the specimen thickness.

## 6. Conclusion

FCG experiments and corresponding macro- and micro-level investigations in this paper indicate that 1) the truncation of low-range loading cycles, in certain levels, leads to significant macro-level crack branching; 2) tension overloads result in subsurface secondary crack irrespective to load truncation level; 3) if there are plenty of low-range loading cycles exist after the tension overload, the secondary crack remains in subsurface, otherwise, it will keep growing to the specimen surface resulting in macro-level crack branching.

## Acknowledgements

The National Natural Science Foundation of China is acknowledged for supporting the project (10802003).

## References

- [1] Alcoa Mill Products: 2324 Aluminium Alloy Plate and Sheet; Website (accessed Aug. 2009): [http://www.alcoa.com/mill\\_products/catalog/pdf/alloy2324-t39techsheet.pdf](http://www.alcoa.com/mill_products/catalog/pdf/alloy2324-t39techsheet.pdf).
- [2] Yamada Y, Newman JC Jr: Int J Fatigue. 31 (2009) 1780-1787.
- [3] Bao R, Zhang X: Int J Fatigue. 32(2010):1180-1189.
- [4] Nesterenko G I, Nesterenko B G: Int J Fatigue. 31 (2009) 1054-1061.
- [5] Frost N E, Marsh K J, Pook L P: *Metal fatigue*. (Clarendon press, Oxford, 1974) pp. 202-292.
- [6] Schijve J: *Fatigue of structures and materials, 2<sup>nd</sup> ed.*.(Springer, 2009) pp 329-372.
- [7] Tian H, Bao R, Zhang J, Zheng X, Fei B: Chinese journal of aeronautics. 22(2009): 401-406.
- [8] Zheng P, Zheng Y, Wei H, Qian Y: Journal of Aeronautical Materials. 14(1994):15-20.
- [9] Derek Hull: *Fractography observing, measuring and interpreting fracture surface topography*. (Cambridge university press) pp.121-155.